

Electronic Supplementary Information

Aluminium Nanoparticles Synthesized by a Novel Wet Chemical Method and Used to Enhance the Performance of Polymer Solar Cells by Plasmonic Effect

Yue Cui,^{a,b,c} Di Huang,^{a,b,†} Yang Li,^{a,b} Wenxiao Huang,^c Zhiqin Liang^{a,b}, Zheng Xu^{a,b}, Suling

Zhao^{a,b,*}

^a Key Laboratory of Luminescence and Optical Information, Beijing Jiaotong University, Ministry of Education, Beijing 100044, PR. China

^b Institute of Optoelectronic Technology, Beijing Jiaotong University, Beijing 100044, PR. China

^c Center for Nanotechnology and Molecular Materials, Department of Physics, Wake Forest University, Winston-Salem, NC, USA

Result and discussion

In order to confirm shell elements around surface, the Fourier transform infrared (FT-IR) spectrum of the prepared Al@PPh₃ NPs were measured. Testing results and structure schematic of PPh₃ are shown in Fig. S1.

(1) C-H vibration of ring hydrogens (marked with triangle)

The peaks at 3066cm⁻¹ and 3001cm⁻¹ are antisymmetrical and symmetrical stretching vibration modes ν_{antisym} and ν_{sym} of C-H stretching.

The peaks at 1178cm⁻¹ and 742cm⁻¹ in fingerprint region are associated with ring deformation vibration τ of the ring C-H wagging.

(2) C-H characteristic pattern (marked with a block)

The weaker peaks between 2000cm⁻¹ and 1660cm⁻¹ are overtone and combination bands of C-H deformation vibrations δ , which are the characteristic pattern for monosubstituted benzene.

(3) Benzene ring vibration (marked the stars)

A resonance at 1581cm⁻¹ is attributed to C-C stretching vibration ν_{sym} , while 1475cm⁻¹ and 1435cm⁻¹ are stretching vibration ν_{antisym} for monosubstituted benzene ring. The peaks at 916cm⁻¹, 852cm⁻¹ and 692 cm⁻¹ are deformation vibration ω of ring.

(4) Phosphorus bond vibration (marked with ring)

Of most interests are strong and medium-intensity bands observed at 1079cm⁻¹, 981cm⁻¹ and 492cm⁻¹ respectively. The bands connect phosphorus and Ph- should appear at 1110cm⁻¹ and 995cm⁻¹ due to the Sadtler handbook of infraed spectra, and we believe that the movement to low wave number is caused by the coordination bond between phosphorus and aluminum ions (showed in Fig. S1b). According to the molecular vibration frequency equation (eq. 1), the wave number σ is proportional to the square root of bond force constant κ .

$$\sigma = \frac{\sqrt{\kappa\mu}}{2\pi c\mu} \quad (1)$$

During the synthesis process, some AlCl₃ molecules stick to the grown Al crystals (confirmed by the EDS analysis). Anhydrous AlCl₃ is a powerful Lewis acid, capable of forming Lewis acid-base adducts with even weak Lewis bases, because of the Al³⁺ ion in the AlCl₃ is the electron-deficient. PPh₃ is a common organophosphorus compound and tends to form a coordination compound for its lone pair electrons. The P ions share the lone pair electrons with AlCl₃ and form a stable coordination compound. The losing of electrons make the P-C bonds force

*Corresponding authors.

Email addresses: slzhao@bjtu.edu.cn

Tel: +86-10-51684462

Address: Institute of Optoelectronics Technology, Beijing Jiaotong University.

constant κ decrease, then lead to a lower wave number. This is consistent with the the FT-IR of P-C bonds at 1079cm^{-1} and 981cm^{-1} . What's more, the coordination compound is confirmed by the appearance of peak at 492cm^{-1} in FT-IR spectrum.

So the existence of PPh_3 shell is clear confirmed by the FT-IR, and these results suggest that the wet chemical process used in our study permits the production of Al@PPh_3 NPs with an PPh_3 layer. Since Al atoms on the surface are bound by coordination bonds with phosphor in PPh_3 , the movement of nanoparticles could be arrested or slowed down. Hence, the physics of burning of Al@PPh_3 NPs stabilized in the organic ligand matrices is expected to be different from free Al@PPh_3 NPs. Meanwhile, the PPh_3 is expected to play dual roles as to prevent aggregation of nano particles or protect it from the oxidation prior to burning because the stereo-hindrance effect caused by PPh_3 molecules on the Al surface block the aggregation in nanoparticles, and lead to a small particle size and stability.

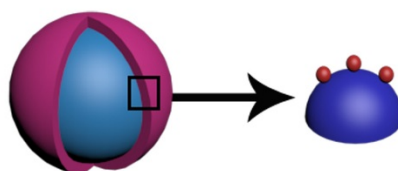
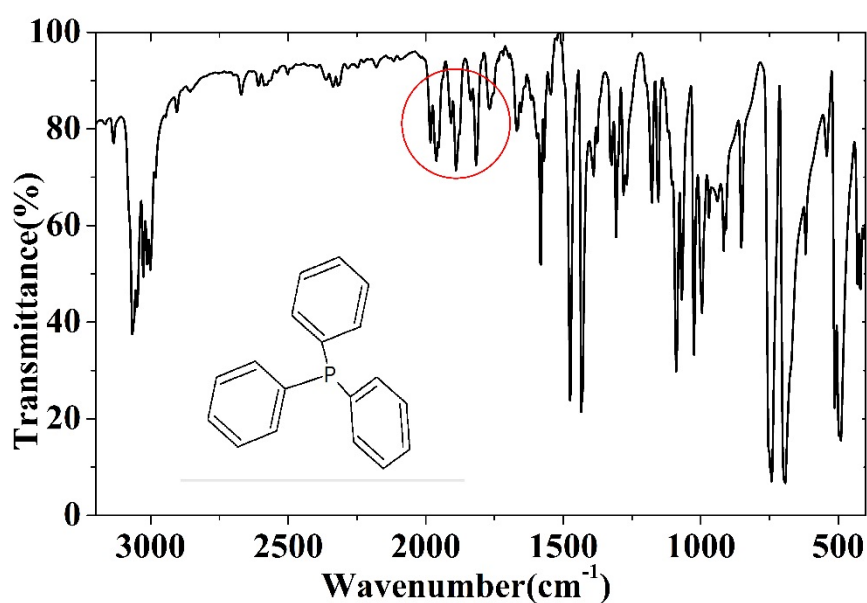


Fig. S1. (a) FTIR spectra of PPh_3 -coated Al@PPh_3 NPs. (b) Schematic illustration of the prepared Al@PPh_3 NPs coated with PPh_3 (purple spheres= Al and Al^{3+} , green sphere= P ions. They are connected by the covalent bond).

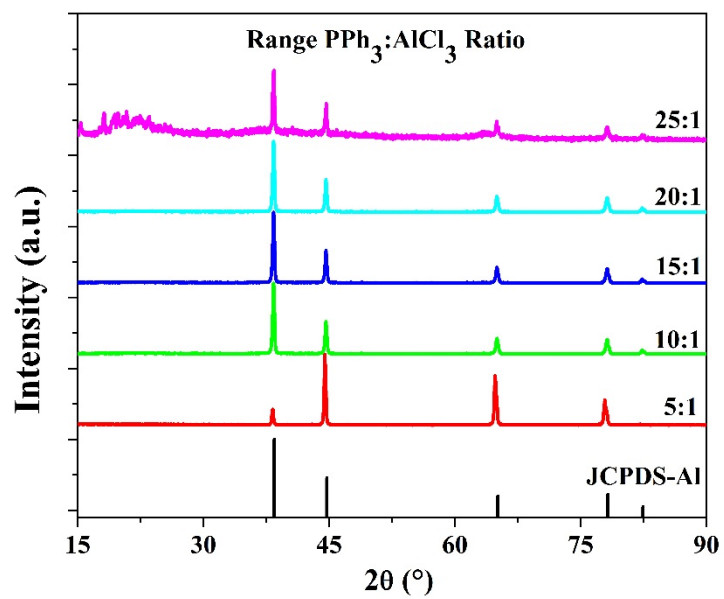


Fig. S2. XRD patterns of prepared Al@PPh₃ NCs in the range of PPh₃:AlCl₃ ratios

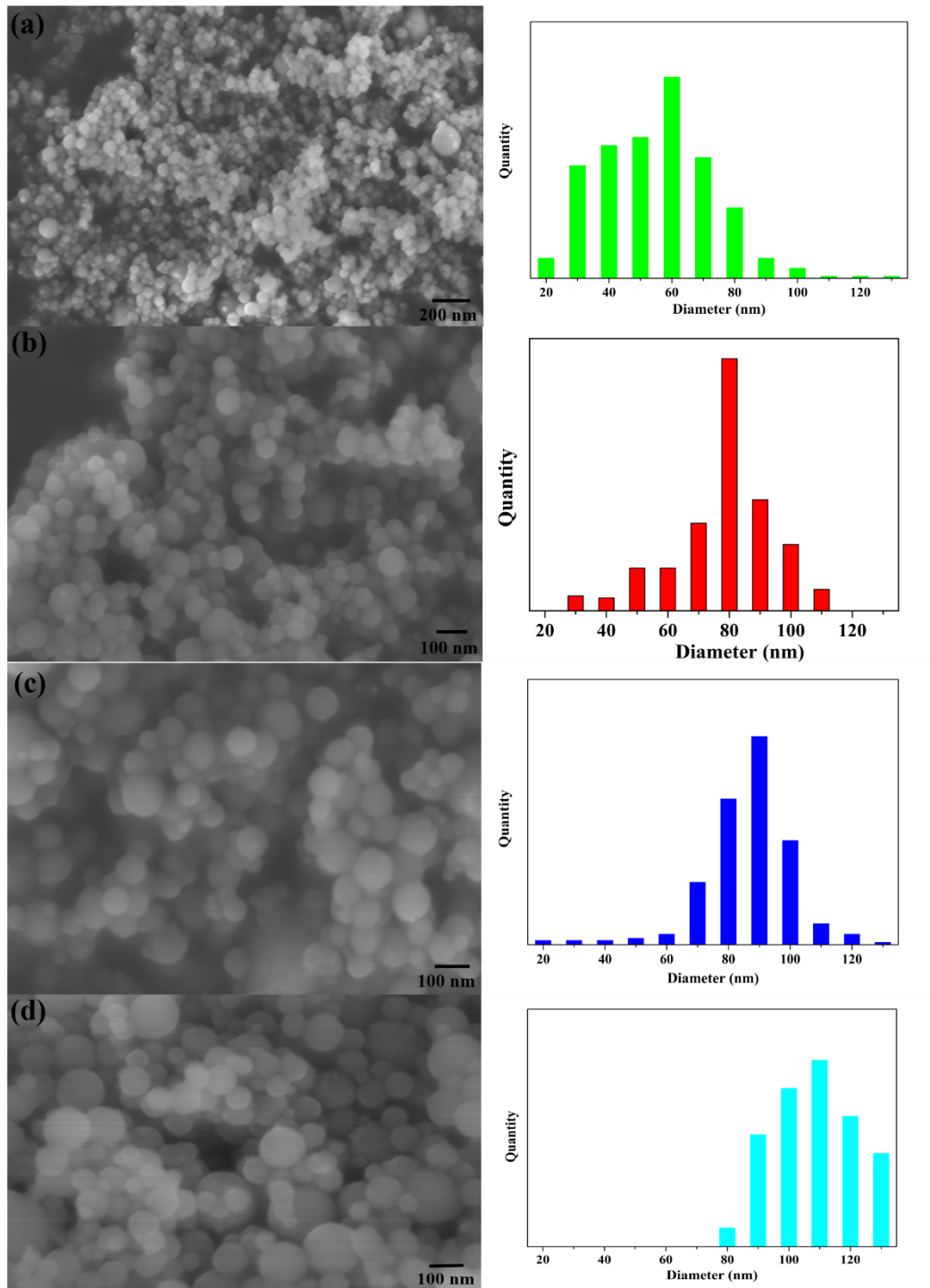


Fig. S3 SEM images and size distribution of prepared Al@ PPh₃ NCs in the range of PPh₃:AlCl₃ ratios. (a) 20:1, (b) 15:1, (c) 10:1, (d) 5:1.

Fig. S2 shows XRD patterns of prepared Al@ PPh₃ NCs in the range of PPh₃:AlCl₃ ratios. We find that high concentration of PPh₃ is bad for crystallizing of NCs, which may be due to the increase in solution viscosity at high PPh₃ concentrations. Higher viscosities can lead to less effective reagent mixing of raw materials. Fig. S3 shows morphology and size distribution of the core-shell nanoparticles. The increasing concentration of PPh₃ lead to the size decrease.

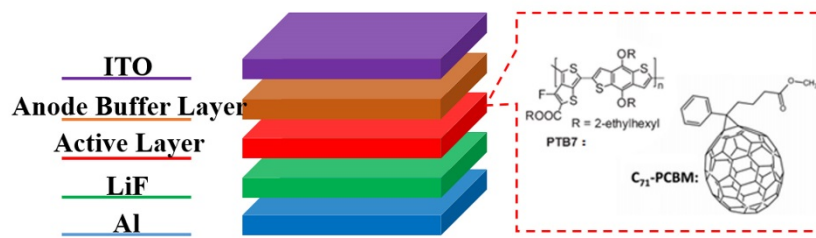


Fig. S4. A schematic structure of PTB7:PC₇₁BM blend PSCs, and the chemical structures of the materials used in the active layer.

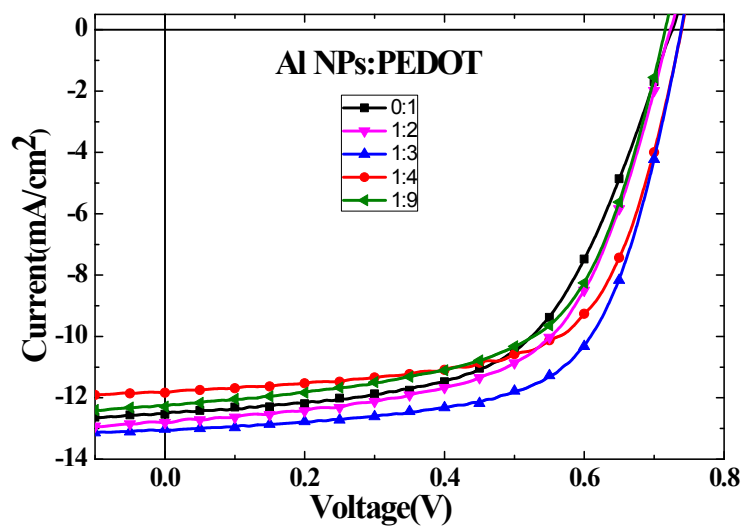


Fig. S5. The J-V characteristic curves of solar cells with different doping ratio of Al NPs

Table S1 Key photovoltaic parameters of solar cells with different doping ratio of Al NPs under AM 1.5 light power of 100 mW/cm²

Doping ratio[Al@PPh ₃ NPs:PEDOT]	V _{oc} [V]	J _{sc} [mA/cm ²]	FF [%]	PCE best [%]
0:1	0.73	12.53	57.5	5.26
1:2	0.72	12.81	60.1	5.54
1:3	0.74	13.02	65.3	6.29
1:4	0.74	11.83	64.8	5.67
1:9	0.72	12.29	59.97	5.30